Available online at www.sciencedirect.com
SCIENCE DIRECT®
Biochemical and Biophysical Research Communications 337 (2005) 160–166
BBRC
www.elsevier.com/locate/ybbrc

# A family 11 xylanase from the pathogen *Botrytis cinerea* is inhibited by plant endoxylanase inhibitors XIP-I and TAXI-I ☆

Alexandre Brutus [a], Ida Barbara Reca [b], Sameh Herga [a], Benedetta Mattei [b], Antoine Puigserver [a], Jean-Claude Chaix [a], Nathalie Juge [a,c], Daniela Bellincampi [b], Thierry Giardina [a,*]

[a] *Institut Méditerranéen de Recherche en Nutrition, Laboratoire de Biochimie et Biologie de la Nutrition, UMR Université Paul Cézanne Aix Marseille III, INRA 1111, service 342, Faculté des Sciences et Techniques Saint-Jérôme, 13397 Marseille Cedex 20, France*
[b] *Dipartimento di Biologia Vegetale, Università di Roma La Sapienza, Piazzale Aldo Moro 5, Rome 00185, Italy*
[c] *Institute of Food Research, Norwich Research Park, Norwich NR4 7UA, UK*

Received 31 August 2005
Available online 15 September 2005

**Abstract**

The phytopathogen fungus *Botrytis cinerea* produces various glycosidases which are secreted during plant infection. In this study, the *XynBc1* cDNA that encodes a xylanase from family 11 glycoside hydrolase from *B. cinerea* was identified by homology-based analysis, cloned by reverse transcription RT-PCR, fully sequenced, and heterologously expressed in *Pichia pastoris* X-33. The purified recombinant protein obtained by chelating-affinity chromatography demonstrated high catalytic activity ($180 \pm 23$ U/mg) and efficiently degraded low viscosity xylan [$K_m = 10 \pm 3$ g $L^{-1}$, $V_{max} = 0.50 \pm 0.04$ μmol xylose $min^{-1}$, and $k_{cat} = 136 \pm 11.5$ $s^{-1}$ at pH 4.5 and 25 °C]. XynBc1 was further tested for its ability to interact with wheat XIP and TAXI type xylanase inhibitors which have been implicated in plant defence. The xylanase activity of XynBc1 produced in *P. pastoris* was strongly inhibited by both XIP-I and TAXI-I in a competitive manner, with a $K_i$ of $2.1 \pm 0.1$ and $6.0 \pm 0.2$ nM, respectively, whereas no inhibition was detected with TAXI-II. We also showed that XynBc1 mRNAs accumulated during early stages of plant tissue infection.


*Keywords:* *Botrytis cinerea*; Xylanase; XIP; TAXI; Cloning; Expression

*Botrytis cinerea* Pers.: Fr.[telomorph: *Botrytina fuckeliana* (de Bary) Wetzel] is a necrotrophic plant pathogen which mainly infects dicotyledons and monocotyledons [1,2]. It causes primarily blossom blights and fruit rots, but can also cause damping-off, bud rot, stem cankers or rots, leaf spots or blights, bulb rots, and tuber or root rots [3–5]. It actively kills plant cells and subsequently lives on killed tissue [6]. *B. cinerea* also causes economic losses on a wide range of cultivated plants, stored fruits, and vegetables. It is one of the most devastating pathogens in several crops worldwide, especially as the major cause for the grey mould disease of grapevine. The mechanisms involved in the infection are still a matter of debate. Various enzymes, i.e., different pectinases and cellulases have been shown to be secreted by the fungus in vitro and in vivo, and may play a role during attack and plant invasion [7]. Xylan is one of the major polysaccharide components of the secondary plant cell walls in cereals. Endo-1,4-β-xylanases (EC 3.2.1.8; xylanases) are produced by plants and microorganisms especially by plant pathogenic fungi and it has been suggested to contribute to infection [8,9].

According to the sequence-based glycoside hydrolase (GH) classification, xylanases are mainly grouped into

☆ *Abbreviations:* XynBc1, xylanase from *Botrytis cinerea* 1; GH, glycoside hydrolase; LVX, low viscosity xylan; TAXI, *Triticum aestivum* xylanase inhibitor; XIP, xylanase inhibitor protein; SPR, surface plasmon resonance.

* Corresponding author. Fax: +33 0 491288440.
*E-mail address:* thierry.giardina@univ.u-3mrs.fr (T. Giardina).

0006-291X/$ - see front matter © 2005 Elsevier Inc. All rights reserved.
doi:10.1016/j.bbrc.2005.09.030

families 10 (GH10) and 11 (GH11) (http://afmb.cnrs-mrs.fr/CAZY/). GH10 family contains plant, fungal, and bacterial enzymes whereas the structurally unrelated GH11 family only includes fungal and bacterial enzymes [10,11]. Here, we report the molecular characterization of *XynBc1* from *B. cinerea* encoding a novel 25 kDa GH11 xylanase expressed during early stage of plant infection. The intronless region of *XynBc1* encoding the predicted mature protein was cloned and expressed in the eukaryotic system *P. pastoris*. This is the first report of a xylanase characterized from the phytopathogen fungus *B. cinerea*. Wheat XIP and TAXI type xylanase inhibitors were shown to specifically interact with the *B. cinerea* xylanase supporting the hypothesis that they are involved in plant defence.

## Materials and methods

*Materials.* The *P. pastoris* expression kit including the *P. pastoris* strain X-33, oligonucleotides, and zeocin were from Invitrogen (Groningen, Netherlands). Restriction endonucleases and DNA modifying enzymes were from Promega (Madison, Wisconsin, USA) and used according to the manufacturer's recommendations. *Pfu* polymerase for polymerase chain reaction (PCR) was from Stratagene (Amsterdam Zuidoost, The Netherlands). *Escherichia coli* DH5 (*supE*44, hsdR17, *recA*1, *endA*1, *gyrA*96, *thi*-1, and *relA*1) was used for DNA manipulation. Dinitrosalicylic acid, (1,4)-β-xylose, and Gamborg B5 were from Sigma–Aldrich; wheat arabinoxylan low viscosity (LVX) was from Megazyme (International Ireland), DyNAzyme was from Finnzymes (Espoo, Finland), and Chelating-Sepharose was from Amersham-Pharmacia Biotech (Uppsala, Sweden).

*Plant material and B. cinerea infection. B. cinerea* B05-10, kindly provided by Prof. Tudzynski (Germany), was grown on potato dextrose agar/yeast extract medium at 20 °C in the dark. Conidia were harvested from a 7-day-old to 8-day-old culture and suspended at a density of $10^6$ conidia/mL in sterile water with 0.5% Tween 20. *Nicotiana tabacum* cv Petit Havana SR1 plant were grown in natural greenhouse.

*Cloning, expression, and purification of XynBc1 in P. pastoris. B. cinerea* was grown on Gamborg B5 media with glucose (0.3% w/v) as unique carbon source. After inoculation at $10^5$/mL, cultures were incubated at 25 °C with shaking (170 rpm) during 2 days. Tobacco plant leaves (~5 cm long) were inoculated with a drop (~10 μL) of this culture at the concentration of $5 \times 10^4$ conidia/μL. Leaves were collected at different times of infection (12, 24, 48, and 72 h), total RNA was isolated with Trizol reagent according to the method of Chomczynski [12,13] and then treated with DNase according to Promega protocol. Total RNA (2 μg) from each sample was used for the reverse transcription reaction in accordance with the manufacturer protocol.

The pPICZαA-derived *P. pastoris* expression plasmid with the cDNA insert encoding XynBc1 was constructed following standard procedures [14]. Total cDNA obtained 24 h after infection was amplified by PCR using the PutXynBc1(5′)w/oPS and PutXynBc1(3′)TAG primers (Table 1) for 40 cycles and at an annealing temperature of 50 °C. The product was purified by the Qiaquick purification kit and ligated into the *Eco*RI/*Xba*I pPICZαA plasmid which was digested with *Sac*I to linearize the DNA for integration into *P. pastoris* genome. The linearized DNA was used for electroporation into *P. pastoris* strain X-33 using a Multiporator (Eppendorf) at 1500 V during 5 ms. Transformants were selected on YPD plates containing 2 μg/μL zeocin. Large-scale expression was achieved as previously described [15]. The culture supernatant was dialysed against the 20 mM Tris/HCl buffer at pH 7.4 overnight. The dialysed sample was loaded onto a Chelating-Sepharose column and eluted with a linear gradient of 0–50 mM EDTA in 20 mM Tris/HCl and 0.5 M NaCl buffer at pH 7.4 and at a flow rate of 2 mL $min^{-1}$. Fractions containing xylanase activity were pooled. The protein concentration was determined using Bradford's method with bovine serum albumin as the standard [16].

*B. cinerea genomic DNA PCR amplification and RT-PCR assay.* Genomic DNA was isolated from *B. cinerea* using the phenol–chloroform extraction method. The PCR was performed as described above with the PutXynBc1(5′)PS and PutXynBc1(3′)w/oTAG as primers (Table 1). The amplification reaction was performed for 40 cycles at an annealing temperature of 50 °C and the resulting PCR product sequenced.

RNA quantification of the target xylanase was performed by PCR on cDNA using two internal primers RT-PutXynBc1(5′) and RT-PutXynBc1(3′). Actin was used as control using the BCactinForward and BCactinRev primers (Table 1) using Applied Biosystem protocol. The amplification reaction was carried out for 40 cycles and at an annealing temperature of 50 °C. Products were separated by 1% agarose gel electrophoresis followed by ethidium bromide.

*Preparation of cell wall fractions.* Cell walls were purified and fractionated as described [17].

*Sequencing and alignment.* Nucleotide and amino acid sequences were identified by the NCBI BLAST search program (http://www.ncbi.nlm.nih.gov/bmlast/). The signal peptide, putative cleavage site, and putative glycosylation sites were predicted using SignalP 3.0 server [18], NetNGlyc 1.0 Server (http://www.cbs.dtu.dk/services/NetNGlyc/), and DictyOGlyc server, respectively (http://www.cbs.dtu.dk/index/shtml/).

*Gel electrophoresis, N-terminal sequencing, and molecular mass determination.* SDS–PAGE was performed in 12% (w/v) polyacrylamide gel as described by Laemmli [19]. N-terminal amino acid sequencing of the Ponceau red-stained protein after electro-transfer on a polyvinylidene difluoride membrane was performed as previously described [20]. Molecular mass determination was performed by electrospray ionization-mass spectrometry (ESI-MS) using a Quattro II instrument (Micromass, Marseille, France) and apomyoglobin as standard.

*Enzyme activity determination, enzyme inhibition assays, and thermal and pH stability.* Xylanase activity, optimal pH, and optimal temperature were measured using the dinitrosalicylic acid (DNS) assay using Low Viscosity Xylan (LVX) as substrate (10 mg $mL^{-1}$), as previously described [15]. The effect of xylanase inhibitors from wheat XIP-I, TAXI-I, and TAXI-II, purified as previously described [21,22], on the activity of XynBc1 was determined on LVX at 30 °C and pH 4.5. The inhibition constant, $K_i$, was calculated for the interaction between XynBc1 and the

Table 1
Primers used in this paper

| Primer names | Sequences |
|---|---|
| PutXynBc(5′)PS | 5′-ATGGTTTCTGCATCTTCCCTCCTCCTCGC-3′ |
| PutXynBc(5′)w/oPS | 5′-TTTAAA**GAATTC**CAAGCCGCGGCACCCGTCAGC-3′ |
| PutXynBc(3′)w/oTAG | 5′-AGAAACAGTGATGGAAGCCGA-3′ |
| PutXynBc(3′)TAG | 5′-TTTAAA**TCTAGA**CTAATGATGATGATGATGATGAGAAACAGTGATGGAAGCCGA-3′ |
| RT-PutXynBC(5′) | 5′-CTCATCGAATACTACATCGT-3′ |
| RT-PutXynBc(3′) | 5′-GTATTGCTTGAAGGTAGCA-3′ |
| BCactinForward | 5′-AAGTGTGATGTTGATGTCC-3′ |
| BCactinRev | 5′-CTGTTGGAAAGTAGACAAAG-3′ |

Letters in bold indicate the restriction site incorporated.

inhibitors (XIP-I and TAXI-I) with different LVX concentrations (0.5%, 0.75%, and 1.0%) and increasing amounts of the inhibitor.

## Results and discussion

### *Identification of a GH11 xylanase cDNA in B. cinerea*

When *B. cinerea* was grown on tobacco cell wall, xylanolytic activity was detected in the supernatant using LVX arabinoxylan as substrate. This result is in agreement with the xylanolytic activity previously reported during plant infection with the fungal pathogen [23]. The *Aspergillus niger* xylanase B (GenBank Accession No. AY536639) was used to search putative GH11 xylanases in the *B. cinerea* (http://www.genoscope.cns.fr/externe/sequences/banque_Projet_DQ). The search revealed a closely related EST sequence (Genoscope databank Accession No.: W0AA061ZB01C1) encoding a protein sequence sharing 56.3% identity at amino acid level with the *A. niger* xylanase. The sequence will be shown to encode a functional xylanase, hereafter named XynBc1. No other cDNA with significant nucleotidic similarity to XynBc1 could be identified in the *B. cinerea* database.

### *Analysis of the XynBc1 nucleotide sequence and RT-PCR assay*

*XynBc1* cDNA was cloned by RT-PCR in pPICZα plasmid and sequencing revealed several differences at posi-

```
1     ATG GTT TCT GCA TCT TCC CTC CTC CTC GCT GCA TCA GCT ATC GCA   45
1     Met Val Ser Ala Ser Ser Leu Leu Leu Ala Ala Ser Ala Ile Ala   15

46    GGT GTC TTC TCC GCG CCA GCC GCG GCA CCC GTC AGC GAG AAC TTG   90
16    Gly Val Phe Ser Ala Pro Ala Ala Ala Pro Val Ser Glu Asn Leu   30

91    AAT GTC TTG CAA GAA AGA GCG TTG ACT TCT TCC GCT ACC GGT ACT   135
31    Asn Val Leu Gln Glu Arg Ala Leu Thr Ser Ser Ala Thr Gly Thr   45

136   AGT GGT GGT TAC TAC TAC TCC TTC TGG ACC GAT GGA AGC GGT GGT   180
46    Ser Gly Gly Tyr Tyr Tyr Ser Phe Trp Thr Asp Gly Ser Gly Gly   60

181   GTT ACA TAC TCC AAC GGA GAC AAT GGT CAA TAT GCC GTA AGC TGG   225
61    Val Thr Tyr Ser Asn Gly Asp Asn Gly Gln Tyr Ala Val Ser Trp   75

226   ACC GGT AAC AAG GGT AAC TTC GTC GGT GGA AAA GGA TGG GCT GTT   270
76    Thr Gly Asn Lys Gly Asn Phe Val Gly Gly Lys Gly Trp Ala Val   90

271   GGT TCC GAG CGG TAA GTT TTT TTT TCC TTC CCT TCG TCA TAC ATG   315
91    Gly Ser Glu Arg --- --- --- --- --- --- --- --- --- --- ---   94

316   AAA AGA CAT CAA ACT AAT TTC TCC CGC AAA G C TCC ATC TCC TAC   361
95    --- --- --- --- --- --- --- --- --- --- -   Ser Ile Ser Tyr   98

362   ACC GGA TCC TAC AAA CCC AAC GGA AAC TCC TAC CTC TCC GTC TAT   406
99    Thr Gly Ser Tyr Lys Pro Asn Gly Asn Ser Tyr Leu Ser Val Tyr   113

407   GGT TGG ACT ACC TTC CCC CTC ATC GAA TAC TAC ATC GTC GAA GAT   451
114   Gly Trp Thr Thr Phe Pro Leu Ile Glu Tyr Tyr Ile Val Glu Asp   128

452   TTT GGC ACC TAC GAT CCC TCC TCC GCC GCC ACC GAA ATC GGC AGT   496
129   Phe Gly Thr Tyr Asp Pro Ser Ser Ala Ala Thr Glu Ile Gly Ser   143

497   GTC ACC TCC GAC GGT TCC ACA TAC AAG ATC CTC GAG ACC ACC CGT   541
144   Val Thr Ser Asp Gly Ser Thr Tyr Lys Ile Leu Glu Thr Thr Arg   158

542   ACA AAC CAA CCT TCC ATT CAA GGA ACT GCT ACC TTC AAG CAA TAC   586
159   Thr Asn Gln Pro Ser Ile Gln Gly Thr Ala Thr Phe Lys Gln Tyr   173

587   TGG TCC GTC CGT ACT AGC AAG CGT ACA AGC GGT ACT GTC ACC ACT   631
174   Trp Ser Val Arg Thr Ser Lys Arg Thr Ser Gly Thr Val Thr Thr   188

632   GCA AAC CAT TTT GCA GCC TGG AAG AAG TTG GGA TTG ACT TTG GGC   676
189   Ala Asn His Phe Ala Ala Trp Lys Lys Leu Gly Leu Thr Leu Gly   203

677   TCA ACC TAC GAC TAC CAA ATT GTT GCT GTT GAG GGT TAC CAA AGC   721
204   Ser Thr Tyr Asp Tyr Gln Ile Val Ala Val Glu Gly Tyr Gln Ser   218

722   AGT GGT TCG GCT TCC ATC ACT GTT TCT TAA                       751
219   Ser Gly Ser Ala Ser Ile Thr Val Ser *                        227
```

Fig. 1. Nucleotide and deduced amino acid sequences of the *XynBc1* gene. Intron is in italic case and the stop codon is marked with an asterisk. The different nucleotides with the Genoscope sequence are in bold. Deduced amino acid sequence is shown below the nucleotide sequence with the putative peptide signal cleavage site marked with an arrow. The different amino acids deduced are in bold. Putative O-glycosylation sites are boxed and putative amino acids implicated in the catalysis are underlined.

tions: 200, 420, 451, 557, 613, 622, 694, and 730 compared to W0AA061ZB01C1 sequence. In addition, it was possible to refine the sequence at positions 662, 671, 686, and 694 where nucleotides were not identified (Fig. 1). The *XynBc1* 684-bp open reading frame resulted in a predicted protein of 227 amino acid residues. This included a 19-amino acid signal peptide, followed by a mature protein of 208 amino acids with a molecular mass of 22,988 Da and a predicted p*I* of 6.27. XynBc1 shares the highest amino acid sequence identity of 66% and 65% with family 11 xylanases from *Phanerochaete chrysosporium*, *Trichoderma reesei*, and *A. kawachi*, respectively (data not shown). The mature XynBc1 protein shows elevated levels of Gly (12.5%), and Ser and Thr (13.9% and 12.5%, respectively). As for *T. viride* xylanase (SwissProt Accession No. Q7Z8Q3), XynBc1 lacks sulphur containing amino acids such as Cys and Met. No potential N-glycosylation site was detected using NetNGlyc 1.0 Server whereas the DictyOGlyc server proposed 2 potential O-glycosylation sites: Ser82 and Ser124.

Analysis of the 751 bp PCR fragment amplified from genomic DNA showed the presence of 2 exons and one intron (Fig. 1). The intron is located after nucleotide 281 of the opening reading frame. The two introns are 281 and 403 bp in length, respectively, and show typical eukaryotic splice site (GT-AG). The organization of the *XynBc1* sequence in the fungal genome was further analysed by Southern blot analysis. Genomic DNA extracted from *B. cinerea* was restricted with *Kpn*I/*Bam*HI and *Kpn*I/*Spe*I. These restriction enzymes do not cut within the *XynBc1* gene whereas *Xho*I cut within the 160 bp gene fragment was used as a probe. The probe hybridized at high stringency with one *Kpn*I/*Bam*HI and *Kpn*I/*Spe*I fragment (250 and 500 bp, respectively) and with two *Xho*I fragments (of 650 and 8000 bp), indicating that *XynBc1* gene is present as a single copy in the fungal genome (data not shown).

The expression of *XynBc1* was investigated by semi-quantitative RT-PCR on total RNA extracted from *B. cinerea* after different infection times on tobacco leaves (12, 24, 48, and 72 h) (Fig. 2). The actin gene from *B. cinerea* (*actA*) was used as an internal control and the intensity of the bands was analysed densitometrically. The ratios of the cDNA amount between of *XynBc1* and *actA*, obtained at each time point, indicated constitutive expression of *XynBc1* during the early stage of infection (data not shown). However, and in accordance with [23], no xylanase activity was present or detectable at the early stages of tobacco leaf infection.

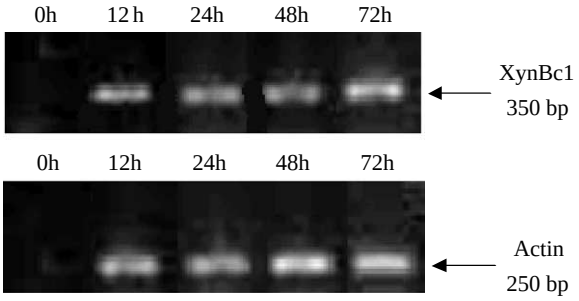


Fig. 2. Expression of *Botrytis cinerea XynBc1* gene during the tobacco infection detected by RT-PCR. The fragment of *XynBc1* amplified was 350 bp and actin was 250 bp.

### *Expression of XynBc1 in P. pastoris*

In order to study the biochemical properties of the xylanase from *B. cinerea*, *XynBc1* cDNA was heterologously expressed in *P. pastoris* using the yeast α mating factor *P. pastoris* signal sequence under the control of the AOX1 promoter. After induction with methanol, a major protein band with an apparent molecular mass of 25 kDa, absent from the supernatant of untransformed cells, was observed in culture filtrate after SDS–PAGE analysis (data not shown). XynBc1 was purified to homogeneity after a single chromatography step (Chelating-Sepharose) where 70% of the total enzymatic activity was recovered. XynBc1 showed

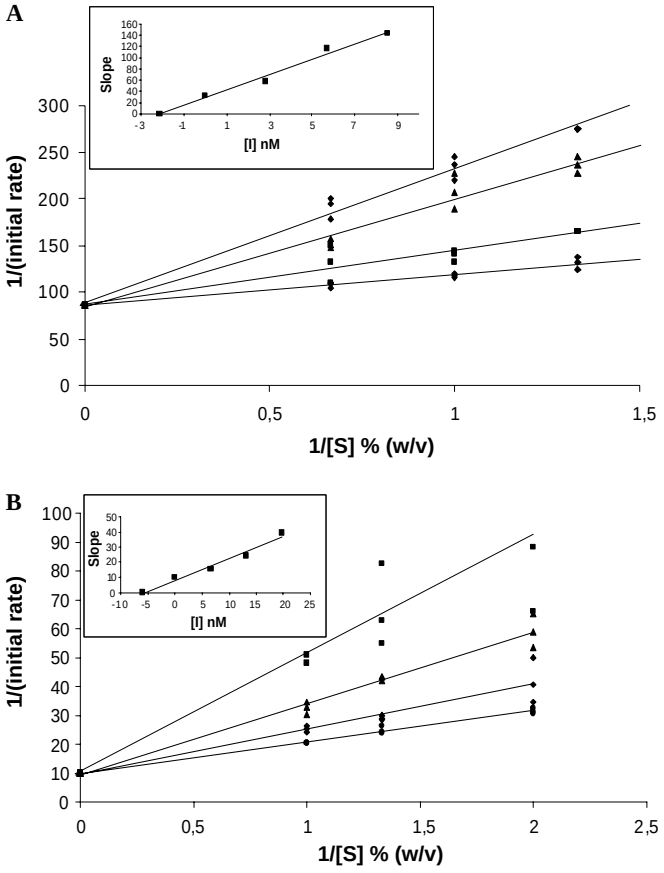


Fig. 3. Kinetic analysis of the inhibition of XynBc1 by XIP-I and TAXI-I using LVX as substrate. The xylanase activity of XynBc1 was determined over a range of substrate concentrations in the absence and presence of known concentrations of (A) XIP-I at 2.9 nM (■), 5.7 nM (▲), and 8.5 nM (♦); (B) TAXI I at 11 nM (■), 16.5 nM (▲), and 27.5 nM (♦). The data are presented as a double reciprocal plot with no inhibitor as control (●). The inset shows a secondary reciprocal plot of the slopes from the primary reciprocal plot versus [XIP-I] or [TAXI I]. Reactions were performed in triplicate.

a single band with an apparent molecular mass of 25,000 Da (data not shown). The $NH_2$-terminal sequencing of the XynBc1 allowed the identification of 7 amino acid residues, Ala-Leu-Thr-Ser-Ser-Ala-Thr, which exactly matched amino acids at position 17–23 of the mature protein, suggesting post-translational proteolysis, as observed for other fungal xylanases [24]. The amino acid differences between our sequence and that reported in the database were confirmed by MALDI-TOF MS peptide mass fingerprinting demonstrating that the two *B. cinera* strains contained different xylanases. Analysis of the protein by mass spectrometry gave a molecular mass of 21,069 Da, indicating the absence of glycosylation of the recombinant enzyme produced in *P. pastoris*, as also confirmed by periodic acid–Schiff staining (data not shown).

### *Enzymatic properties of recombinant XynBc1 and enzyme inhibition by wheat xylanase inhibitors*

The specific activity of recombinant XynBc1 using low viscosity xylane (LVX) as substrate was $180 \pm 23$ U $mg^{-1}$. The effects of pH and temperature on the enzymatic activity were investigated on the recombinant enzyme. XynBc1 displayed optimum activity in the 4.5–5.0 pH range whereas the activity was lost at pH 2.5. At pH 4.5, the optimal enzymatic activity was observed between 38 and 42 °C whereas the activity drastically decreased above 45 °C. The recombinant enzyme was stable at 35 °C for 30 min but the activity was radically affected at 40 °C. In fact, only 20% of the activity remained after 10 min of incubation at this temperature (data not shown). From sequence comparison of XynBc1 with other related fungal GH11 xylanases with known three-dimensional structures (http://afmb.cnrs-mrs.fr/CAZY/) (Fig. 4), $Glu103_{XynBc1}$ and $Glu195_{XynBc1}$ catalytic residues are invariant. These residues, suitably located in the active site cleft, are putatively involved in the formation of the α-glycosyl-enzyme intermediate where Glu103 can act as a general acid catalyst by protonating the substrate, while Glu195 performs a nucleophilic attack which results in the departure of the leaving group and the formation of the intermediate.

The apparent kinetic parameters of XynBc1 were determined using LVX at pH 4.5 and 25 °C. XynBc1 showed a $K_m$ of $10 \pm 3$ g $L^{-1}$ and a $k_{cat}$ of $136 \pm 11.5$ $s^{-1}$. The interaction between XynBc1, and XIP-I and TAXI-I, two types of xylanase inhibitors with no structural homology, was analysed by surface plasmon resonance (SPR) to determine the dissociation constant ($K_D$) for the interaction between XynBc1 and wheat inhibitors, XIP-I and TAXI-I. Either XynBc1 or the xylanase inhibitors were covalently linked to the sensor chip. In both cases, the interaction was irreversible and different attempts to displace the bound protein to regenerate the sensor chip were unsuccessful, preventing the determination of a $K_D$ value. The kinetics of inhibition of XynBc1 by XIP-I and TAXI-I were determined by enzymatic assay in solution using LVX arabin-

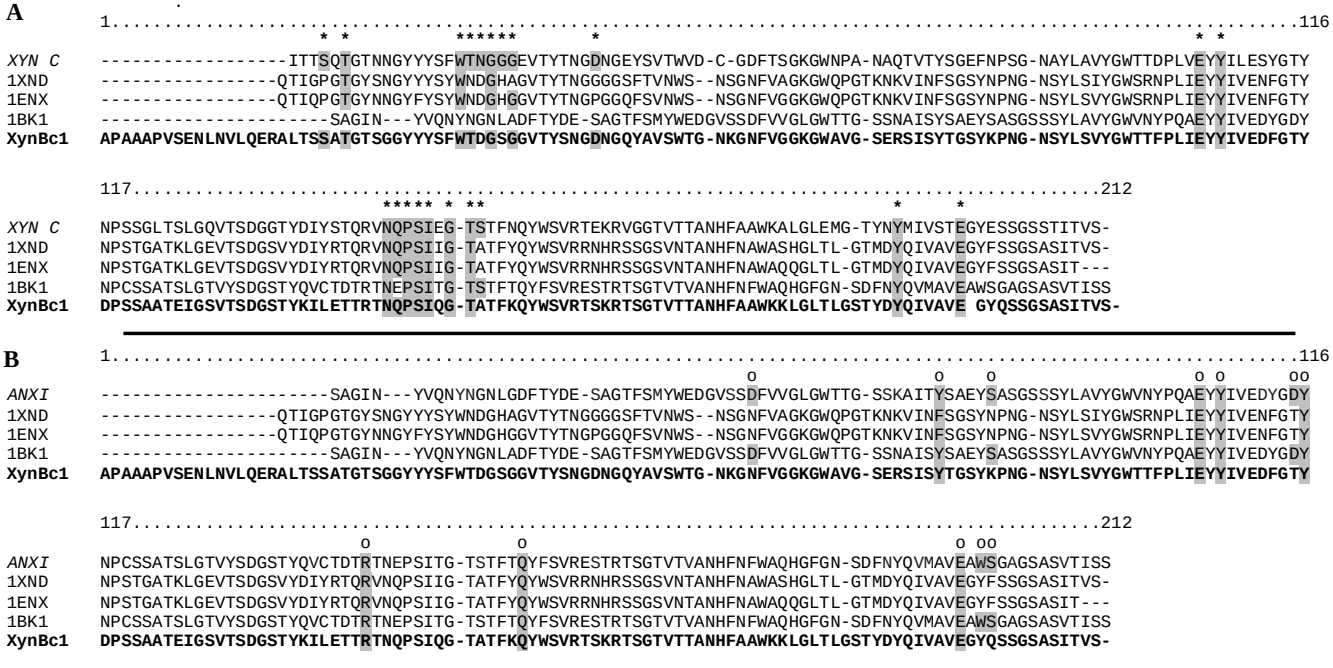


Fig. 4. Multiple alignments of GH 11 xylanases from different fungi. The sequences are referenced with the corresponding GenBank or SwissProt accession numbers. Figure was prepared with Bioedit [30]. XynBc1 sequence, represented in bold, was aligned with: *Trichoderma harzianum* (1XND: P48793), *Trichoderma reesei* xylanase 2 (1ENX: P36217), and *Aspergillus kawachii* (1BK1: P33557). (A) The alignment also including *Penicillium funiculosum* xylanase C (XYNC: Q9HFH0), the fungal xylanase co-crystallized with XIP-I [25]. Stars (∗) show XYNC residues interacting with XIP-I and among which in grey are indicated amino acid identities. (B) An alignment also including *Aspergillus niger* xylanase 1 (ANXI: P55329), the fungal xylanase co-crystallized with TAXI-I. Circles (○) show ANXI residues interacting with TAXI-I and among which in grey are indicated amino acid identities [26].

oxylan as substrate. In the presence of the inhibitor, the $V_{max}$ did not change while the $K_m$ increased with increasing the concentrations of the inhibitor protein, indicating a competitive mode of inhibition both for XIP-I and TAXI-I (Figs. 3A and B). A competitive inhibition is consistent with the three-dimensional structures of the complexes between *P. funiculosum* xylanase C (XYNC) and *A. niger* xylanase (ANX1) with the inhibitors XIP-I [25] and TAXI-I [26], respectively. A similar mode of inhibition had been observed for PGIP, a protein inhibitor of fungal polygalacturonases [27,28], and for PMEI, a protein inhibitor of plant pectin methylesterase [29], suggesting that this may represent a general strategy evolved by plants for controlling cell wall degrading enzymes. The secondary plot of slope against inhibitor concentration gave an inhibition constant $K_i$ of $2.1 \pm 0.1$ nM for XIP-I and $6.0 \pm 0.2$ nM for TAXI-I (Fig. 3). Interestingly, no inhibition was detected with TAXI-II, as previously reported for this inhibitor with xylanases produced by *A. niger* [22] and *P. funiculosum* (XYNB) [15]. The alignment of XynBc1 with fungal GH11 xylanases revealed that the residues important for the interaction of XYNC with XIP-I and ANX1 with TAXI-I are mostly conserved in XynBc1 (Fig. 4).

To the best of our knowledge, this is the first characterization of a xylanase gene from the phytopathogen *B. cinerea*. Xylanases are produced by a number of plant pathogenic fungi and it has been suggested that they may contribute to infection, although the mechanism of action remains to be determined. Targeted disruption of xylanase genes was carried out without any significant conclusion on their pathogenic importance [9], maybe because, phytopathogens secrete numerous different xylanases and it is difficult to abolish completely the activity. In the present study, we showed that *B. cinerea* produces xylanase during plant tissue infection, reinforcing a role for this type of enzyme in the plant attack. In addition, the *B. cinerea* xylanase is inhibited by XIP-I and TAXI-I, two wheat proteins believed to be involved in plant defence against pathogens and whose expression is induced by fungal pathogens such as *Erysiphe graminis* and *Fusarium graminearum* as well as abiotic stress signals [31,32].

We have demonstrated the inhibition performed by XIP-I of a xylanase produced by a fungal pathogen during the first stages of infection. It remains to be investigated to what extent the interaction between fungal xylanases and specific inhibitors actually contribute to plant defence in planta.

## Acknowledgments

We thank Drs. Tariq Tahir and Kurt Gebruers for providing xylanase inhibitors. We also thank Drs. Daniela Pontiggia and Cinzia Manfredini for providing cell wall materials, RNA from infected leaves, and technical help. This study has been carried out with the financial support from the Commission of the European Communities, under the specific program for RTD and Demonstration on "Quality of Life and management of living resources," Key Action 1-Food, Nutrition and Health, Contract: QLK1-2000-00811 GEMINI "Solving the problem of glycosidase inhibitors in food processing." A.B. acknowledges French and Italian governments to the bilateral grant obtained under the reference "DM3935."

## References

[1] I. Gudelj, B.D.L. Fitt, F. van den Bosch, Evolution of sibling fungal plant pathogens in relation to host specialization, Phytopathology 94 (2004) 789–795.
[2] J. Hubert, V. Stejskal, Z. Munzbergova, A. Kubatova, M. Vanova, E. Zdarkova, Mites and fungi in heavily infested stores in the Czech Republic, J. Econ. Entomol. 97 (2005) 2144–2153.
[3] M.K. Hausbeck, G.W. Moorman, Managing *Botrytis* in greenhouse-grown flower crops, Plant Dis. 80 (1996) 1212–1219.
[4] W.G. Kim, W.D. Cho, Developmental characteristics of gray mold in pepper, J. Agric. Sci. Crop Protect. 38 (1996) 466–472.
[5] L.E. Sweets, F.L. Pfleger, F.C. Morgan, J.R. Mizicko, Control of fungi associated with cankers of greenhouse roses, Plant Dis. 66 (1982) 491–494.
[6] W.R. Jarvis, *Botryotinia and Botrytis* species: Taxonomy, Physiology and Pathogenicity, A guide to the literature, Tech. Rep. Res. Branch, Can. Dep. Agric. Monog. No. 15, 1977.
[7] R.P. Doss, Composition and enzymatic activity of the extracellular matrix secreted by germlings of *Botrytis cinerea*, Appl. Environ. Microbiol. 65 (1999) 404–408.
[8] E. Gomez-Gomez, M.C. Ruiz-Roldan, A. Di Pietro, M.I. Roncero, C. Hera, Role in pathogenesis of two endo-beta-1,4-xylanase genes from the vascular wilt fungus *Fusarium oxysporum*, Fungal Genet. Biol. 35 (2002) 213–222.
[9] J.D. Walton, Deconstructing the cell wall, Plant Physiol. 104 (1994) 1113–1118.
[10] Y. Bourne, B. Henrissat, Glycoside hydrolases and glycosyltransferases: families and functional modules, Curr. Opin. Struct. Biol. 11 (2001) 593–600.
[11] B. Henrissat, A classification of glycosyl hydrolases based on amino acid sequence similarities, Biochem. J. 280 (1991) 309–316.
[12] P. Chomczynski, N. Sacchi, Single-step method of RNA isolation by acid guanidinium thiocyanate–phenol–chloroform extraction, Anal. Biochem. 162 (1987) 156–159.
[13] P. Chomczynski, K. Mackey, Short technical reports. Modification of the TRI reagent procedure for isolation of RNA from polysaccharide- and proteoglycan-rich sources, Biotechniques 19 (1995) 942–945.
[14] J. Sambrook, E.F. Fritsch, T. Maniatis, Cloning: A Laboratory Manual, second ed., Cold Spring Harbor Laboratory Press, Cold Spring Harbor, NY, 1989.
[15] A. Brutus, C. Villard, A. Durand, T. Tahir, C. Furniss, A. Puigserver, N. Juge, T. Giardina, The inhibition specificity of recombinant *Penicillium funiculosum* xylanase B towards wheat proteinaceous inhibitors, Biochim. Biophys. Acta—Proteins Proteom. 1701 (2004) 121–128.
[16] M.M. Bradford, A rapid and sensitive method for the quantitation of microgram quantities of protein utilizing the principle of protein-dye binding, Anal. Biochem. 72 (1976) 248–254.
[17] T. Stolle-Smits, J.G. Beekhuizen, C. Van Dijk, A.G.J. Voragen, K. Recourt, Cell wall dissolution during industrial processing of green beans (*Phaseolus vulgaris* L.), J. Agric. Food Chem. 43 (1995) 2480–2486.
[18] H. Nielsen, J. Engelbrecht, S. Brunak, G. von Heijne, Identification of prokaryotic and eukaryotic signal peptides and prediction of their cleavage sites, Protein Eng. 10 (1997) 1–6.
[19] U.K. Laemmli, Cleavage of structural proteins during the assembly of the head of bacteriophage T4, Nature 227 (1970) 680–685.

[20] P. Matsudaira, Sequence from picomole quantities of proteins electroblotted onto polyvinylidene difluoride membranes, J. Biol. Chem. 262 (1987) 10035–10038.
[21] R. Flatman, W.R. McLauchlan, N. Juge, C.S. Furniss, J.G. Berrin, R.K. Hughes, P. Manzanares, J.E. Ladbury, R. O'Brien, G. Williamson, Interactions defining the specificity between fungal xylanases and the wheat proteinaceous inhibitor, XIP-I, Biochem. J. 365 (2002) 773–781.
[22] K. Gebruers, W. Debyser, H. Goesaert, P. Proost, J. Van Damme, J.A. Delcour, *Triticum aestivum* β endoxylanase inhibitor (TAXI) consist of two inhibitors, TAXI I and TAXI II, with different specificities, Biochem. J. 353 (2001) 239–244.
[23] A. Tiedemann, Evidence for a primary role of active oxygen species in induction of host cell death during infection of bean leaves with *Botrytis cinerea*, Physiol. Mol. Plant Pathol. 50 (1997) 151–166.
[24] J.F.D. Dean, J.D. Anderson, Ethylene biosynthesis-inducing xylanase: II. Purification and physical characterization of the enzyme produced by *Trichoderma viride*, Plant Physiol. 95 (1991) 316–323.
[25] F. Payan, P. Leone, S. Porciero, C. Furniss, T. Tahir, G. Williamson, A. Durand, P. Manzanares, H.J. Gilbert, N. Juge, A. Roussel, The dual nature of the wheat xylanase protein inhibitor XIP-I: structural basis for the inhibition of family 10 and family 11 xylanases, J. Biol. Chem. 279 (2004) 36029–36037.
[26] S. Sansen, C.J. De Ranter, K. Gebruers, K. Brijs, C.M. Courtin, J.A. Delcour, A. Rabijns, Structural basis for inhibition of *Aspergillus niger* xylanase by *Triticum aestivum* xylanase inhibitor-I, J. Biol. Chem. 279 (2004) 36022–36028.
[27] G. De Lorenzo, R. D'Ovidio, F. Cervone, The role of polygalacturonase-inhibiting proteins (PGIPs) in defense against pathogenic fungi, Annu. Rev. Phytopathol. 39 (2001) 313–335.
[28] A. Di Matteo, L. Federici, B. Mattei, G. Salvi, K.A. Johnson, C. Savino, G. De Lorenzo, D. Tsernoglou, F. Cervone, The crystal structure of polygalacturonase-inhibiting protein (PGIP), a leucine-rich repeat protein involved in plant defense, Proc. Natl. Acad. Sci. USA 100 (2003) 10124–10128.
[29] A. Di Matteo, A. Giovane, A. Raiola, L. Camardella, D. Bonivento, G. De Lorenzo, F. Cervone, D. Bellincampi, D. Tsernoglou, Structural basis for the interaction between pectin methylesterase and a specific inhibitor protein, Plant Cell 17 (2005) 849–858.
[30] T.A. Hall, BioEdit: a user-friendly biological sequence alignment editor and analysis program for Windows 95/98/NT, Nucleic Acids Symp. Ser. 41 (1999) 95–98.
[31] T. Igawa, T. Ochiai-Fukuda, N. Takahashi-Ando, S. Ohsato, T. Shibata, I. Yamaguchi, M. Kimura, New TAXI-type xylanase inhibitor genes are inducible by pathogens and wounding in hexaploid wheat, Plant Cell Physiol. 45 (2004) 1347–1360.
[32] T. Igawa, T. Tokai, T. Kudo, I. Yamaguchi, M. Kimura, A wheat xylanase inhibitor gene, xip-I, but not taxi-I, is significantly induced by biotic and abiotic signals that trigger plant defense, Biosci. Biotechnol. Biochem. 69 (2005) 1058–1063.